Polymeric Multilayer Films Comprising Deconstructible Hydrogen-Bonded Stacks Confined between Electrostatically Assembled Layers

Jinhan Cho[†] and Frank Caruso*[,†]

Max Planck Institute of Colloids and Interfaces, D-14424 Potsdam, Germany

Received July 3, 2002

ABSTRACT: Deconstructible polymeric films have potential applications in the areas of drug delivery, patterning, and membrane science. Here, we report on the preparation of heterogeneous multilayer films comprising alternate stacks of hydrogen-bonded (poly(4-vinylpyridine) (P4VP) and poly(acrylic acid, sodium salt) (PAA)) and electrostatically formed (poly(sodium 4-styrenesulfonate) (PSS) and poly(allylamine hydrochloride) (PAH)) layers via the layer-by-layer (LbL) assembly technique. We demonstrate that these polymeric films are highly pH sensitive toward deconstruction, with the onset of film deconstruction occurring at about pH 7.4. The pH-induced film deconstruction characteristics (total film loss and rate of deconstruction) depend on the number of hydrogen-bonded layers $(PAA/P4VP)_n/PAA$ inserted between stacks of PAH/PSS layers. Films containing a single hydrogen-bonded trilayer stack ($n = 1$) confined between PAH/PSS layers are stable up to pH 8.5, with only 15 wt % of the film desorbed at pH 10.3. Corresponding (nonconfined) PAA/P4VP films completely deconstruct (100% film loss) at this pH, indicating that the film deconstruction characteristics are closely related to the extent of physical confinement provided by the electrostatically assembled polyelectrolyte layers. Increasing the number of physically confined hydrogen-bonded layers in the film results in a systematic and significant increase in film loss from 15 ($n = 1$) to 83 wt % ($n = 4$) at pH 10.3. The current approach represents a facile means to tailor the deconstruction rates of polymeric multilayer films through the pH sensitivity of PAA/P4VP layers.

Introduction

Ultrathin polyelectrolyte (PE) multilayer films constructed by the versatile layer-by layer (LbL) assembly method have been utilized for the preparation of light-emitting diodes,[1−6] and electrochromic,[7,8] membrane,[9−13] and bioactive enzyme thin films,[14−16] as well as for selective area patterning[17−20] and particle surface modification.[21−27] Since the introduction of the LbL technique in 1991 by Decher and Hong,[28] numerous polycation and polyanion pairs have been used to form multilayer films through electrostatic interactions,[29] with commonly one of the film components being a strong polyelectrolyte. More recently, however, the assembly of films from weak PEs have attracted considerable interest, largely because of their pH dependent characteristics.[30−35] For example, Rubner and co-workers have reported that the pH of the dipping solution has a significant effect on the surface morphology, film thickness, surface wettability, and interpenetration of poly(allylamine hydrochloride) (PAH)/poly(acrylic acid, sodium salt) (PAA) multilayer films due to changes in the ionization degree of the weak PEs.[30−32] The observation that PAA adsorbed onto PAH has a higher degree of ionization than PAA in bulk solution has initiated studies focusing on the local electrostatics[34,35] and charge density of weak PE films.[30−32] Multilayers of weak PEs have also been used to form thin nanoporous[33] and microporous[32] films and have been exploited as nanoreactors for the synthesis of metallic nanoparticles.[36]

Hydrogen-bonding interactions constitute an alternative driving force for fabricating multilayer films of weak PEs.[37−41] Previous investigations have shown that multilayers composed of hydrogen-bonded weak PE layers are very sensitive to pH changes due to the generation of electrostatic repulsion between layers within the films.[40,41] For example, Sukhishvili and Granick have recently reported that hydrogen-bonded multilayer films containing a weak PE, for example PAA/poly(ethylene oxide) (PEO) or poly(methacrylic acid)/poly(vinylpyrrolidone) films, can be completely erased (or deconstructed) at pH 3.6 and 6.9, respectively.[40,41] More recently, it was demonstrated that hydrogen-bonded multilayer films of PAA and poly(acrylamide) (PAAm) are highly stable at pH 7 after cross-linking the PAA and PAAm layers by thermal or photoinduced treatment.[42] These findings clearly suggest the possibility of using hydrogen-bonded multilayer films based on weak PEs in applications such as micropatterning and drug delivery, where control of the deconstruction rate of the hydrogen-bonded films is desirable. One approach to modulating the deconstruction behavior of multilayered thin films is via structural design of the films. As it is well established that PE multilayers comprise networks of interpenetrated polymer chains,[29] physically confining deconstructible layers within stacks of stable PE layers is expected to have a significant influence on the film deconstruction properties.

In this study, we investigate the pH stability and pH-induced deconstruction kinetics of multilayer films comprised of physically confined (i.e., sandwiched) hydrogen-bonded (PAA/poly(4-vinylpyridine) (P4VP)) (P_H) layers between electrostatically assembled PAH/poly(sodium 4-styrenesulfonate) (PSS) (PE_E) stacks. PAA was employed as a polymeric bridge between the

* To whom correspondence should be addressed.
[†] Present address: Department of Chemical and Biomolecular Engineering, The University of Melbourne, Victoria 3010, Australia. Fax: (+61) 3 8344 4153. E-mail: fcaruso@unimelb.edu.au.

10.1021/ma021049n CCC: $25.00
Published on Web 03/29/2003

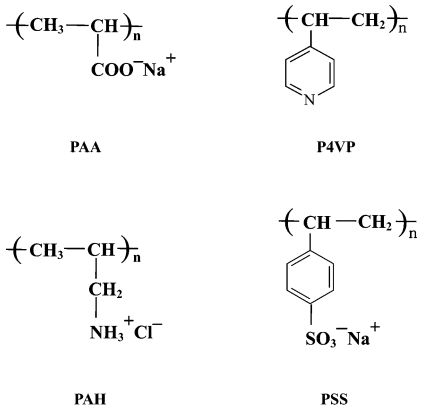

Figure 1. Chemical structures of the polymers used.

different types of layer stacks (i.e., P_H and PE_E) to promote multilayer film formation. It is shown that the approach outlined can be used to prepare, at one end, films that are pH resistant over a broad pH range and, on the other, highly pH sensitive, deconstructible films by exploiting the pH sensitivity of hydrogen-bonded layers. Furthermore, the deconstruction kinetics and the desorbed amount of the multilayer films can be controlled, without any chemical modification of the films required.

Experimental Section

Materials. Poly(sodium 4-styrenesulfonate) (PSS) ($M_w \sim 70\,000$), poly(allylamine hydrochloride) (PAH) ($M_w \sim 70\,000$), poly(acrylic acid, sodium salt) (PAA) ($M_w \sim 2100$), and poly(4-vinylpyridine) (P4VP) ($M_w \sim 60\,000$) were used as received from Aldrich. The structures of the polymers used are shown in Figure 1. Quartz substrates were purchased from Hellma Optik GmbH (Jena, Germany) and QCM electrodes were obtained from Kyushu Dentsu (Nagasaki, Japan). All deposition and rinse solutions used for the buildup of multilayer films were a mixture of water and methanol (50/50 v/v %) and their pH was adjusted to 3.5 with 0.1 M HCl. The quartz slides were cleaned by treatment with piranha solution (sulfuric acid/hydrogen peroxide = 70/30 v/v %) and subsequently charged negatively by heating at 70 °C for 20 min in a 5:1:1 vol %. mixture of water, hydrogen peroxide, and 29% ammonia solution. Water from a three-stage USF Purelab Plus purification system with a resistivity greater than 18 MΩ cm^{-1} was used in all experiments.

Preparation of Multilayer Films. The concentration of polymer solutions used for all experiments was 10 mM (with respect to the monomer unit). No salt was added to the solutions. The quartz substrates were first dipped for 20 min in the cationic PAH solution, then washed three times in a water/methanol (50/50 v/v %) mixture of pH 3.5 by dipping for 2 min, followed by drying with a gentle stream of nitrogen.[38,39] PSS, PAH, and PAA layers were sequentially deposited onto the substrates using the same washing and drying procedure as described above. PAA and P4VP form layers through hydrogen-bonding interaction between the carboxylic acid and pyridine groups on the polymers, respectively. The outermost layer of the hydrogen-bonded layers was always PAA so that the films could be readily capped with additional PE layers (e.g., PAH/PSS/PAH) through electrostatic interactions. Four different sample series were prepared with hydrogen-bonded layers confined between multilayers that were assembled through electrostatic interactions. The number of PAA/P4VP bilayers separating each PAH/PSS/PAH trilayer was varied from 1 to 4. The corresponding samples are denoted as $PE_E/(P_H)_1$/PAA/PE_E, $PE_E/(P_H)_2$/PAA/PE_E, $PE_E/(P_H)_3$/PAA/PE_E, and $PE_E/(P_H)_4$/PAA/PE_E, respectively, where PE_E = PAH/PSS/PAH and $(P_H)_n$ = (PAA/P4VP)$_n$, $n = 1 \sim 4$.

Fourier Transform Infrared Spectroscopy (FTIR). FTIR spectra were taken with a FTIR-200 spectrometer (JASCO Corporation). Calcium fluoride (CaF_2) substrates dipped in a poly(ethylenimine) solution of 1 wt % for 30 min were used, and then P4VP films were spin-coated onto the substrates at 3000 rpm. To investigate the degree of protonation of P4VP depending on the pH, we prepared three different solutions: P4VP dissolved in pure methanol and P4VP in water/methanol (50/50 vol %) mixtures of pH 3.5 and 1.8.

Ellipsometry. The thicknesses of the P4VP/PAA multilayer films were determined from data recorded with a L2W16C830 (Gaertner) ellipsometer. These multilayer films were formed onto PEI-coated silicon wafers. The refractive index was allowed to vary in fitting the ellipsometric data using an iterative process.

UV−Vis Spectrophotometry. UV−vis spectra were taken with a HP5453 UV−vis spectrophotometer. PSS and P4VP show absorbance peaks centered at 225 and 256 nm, respectively.

Quartz Crystal Microgravimetry. A QCM device was used to investigate the mass deposited after each adsorption step.[43] The resonance frequency of the QCM electrodes was ca. 9 MHz. Assuming the film density of PEs and P4VP used in our study is 1.2×10^{-6} g m^{-3},[36] the PE film thickness, d, can be calculated from the change in QCM frequency, ΔF, according to the equation Δd (nm) = − 0.017ΔF (Hz).[43,44]

Results and Discussion

We first investigate the sequential growth and the pH stability of hydrogen-bonded (PAA/P4VP) multilayer films, followed by the formation of heterogeneous multilayers composed of hydrogen-bonded layers inserted between electrostatically assembled PAH/PSS stacks, and the pH stability of these films.

Preparation and Deconstruction of Hydrogen-Bonded Multilayer Films. Weak PE PAA chains carry a majority of carboxylic acid (−COOH) groups for hydrogen-bonding interactions at low pH (pH < 2.5),[32,42] and carboxylate ions ($-COO^-$) for electrostatic interactions at high pH (pH > 7).[32] Therefore, by appropriately adjusting the pH of the PAA deposition solution, the two different forms can coexist in PAA at the same time, giving rise to both electrostatic (by $-COO^-$) and hydrogen-bonded (by −COOH) interactions.

QCM frequency changes, ΔF, show that regular multilayer film growth occurs when PAA and P4VP are LbL assembled from a water/methanol mixture (50/50 v/v %) of pH = 3.5 (Figure 2a). This solvent combination was chosen to provide enhanced stability for the multilayers (see later). The alternate deposition of PAA and P4VP results in a $-\Delta F$ of 180 and 110 Hz, respectively. The average layer thicknesses calculated from these QCM data are 3.1 nm for PAA and 1.9 nm for P4VP. Although both COOH and COO^- groups can coexist in PAA at pH = 3.5, P4VP is only slightly protonated under the conditions used for assembly (pH 3.5). Hence, the interactions between the PAA and P4VP layers are mainly due to hydrogen bonding (see later).[35,45] The relative ratio of COOH (peak centered at 1709 cm^{-1}) and COO^- (centered at 1570 cm^{-1}) of PAA in the PAA/P4VP multilayer films was not investigated by Fourier transform infrared (FTIR) due to the strong absorption peaks (ring vibration) of the pyridine groups of P4VP at 1595 and 1556 cm^{-1}, which result in masking of the COO^- peak of PAA.[38,39] However, based on FTIR analysis of a PAA solution, less than 10% of PAA is ionized at pH = 3.5[32,40,41] (The role of the COO^- groups of PAA for electrostatic layer buildup will be briefly discussed in the following section.) Furthermore, as shown in Figure 2b, the FTIR analysis of absorbance peaks contributing from unprotonated (centered at 1600

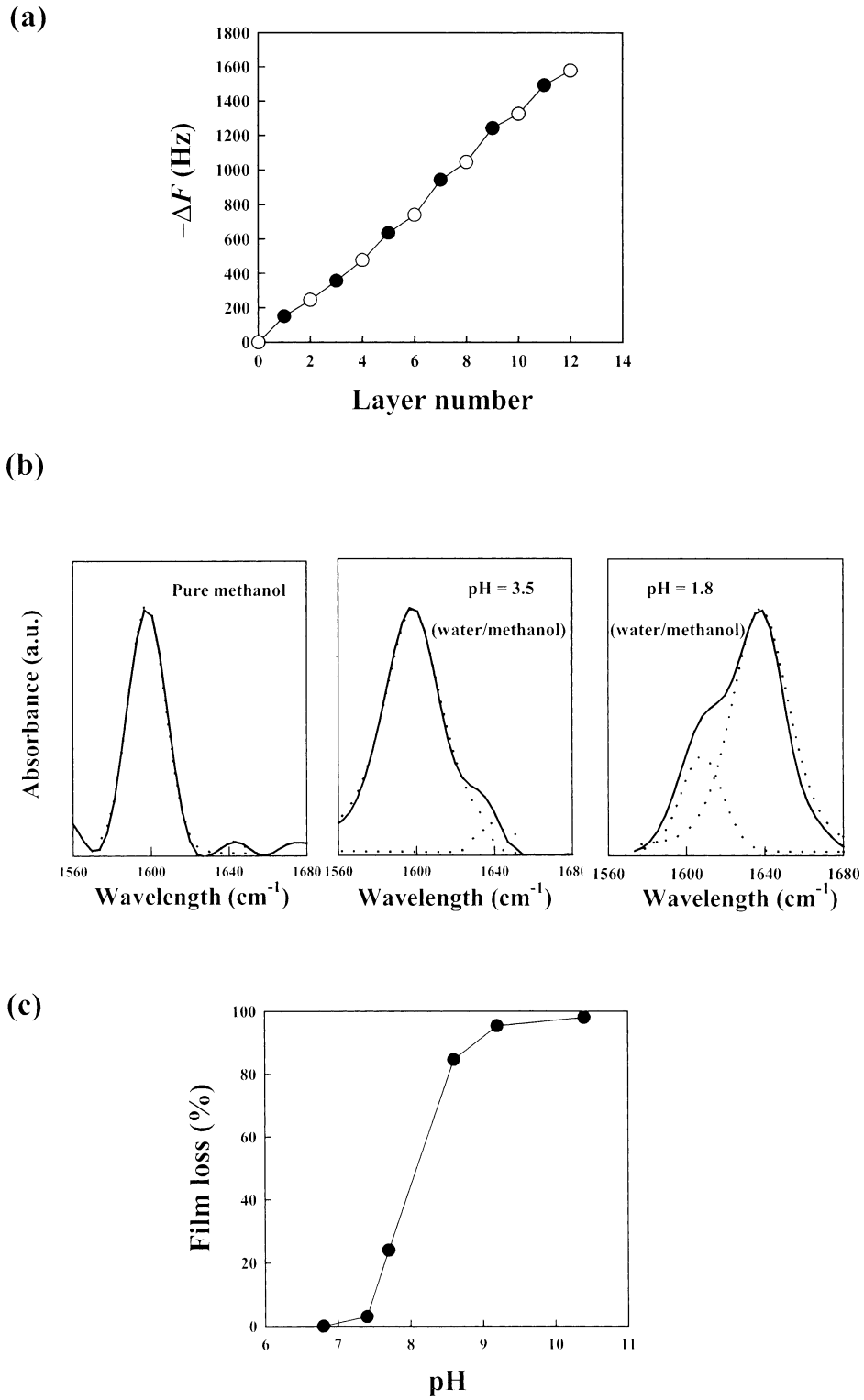

Figure 2. (a) QCM frequency change as a function of layer number for the assembly of PAA (filled circles) and P4VP (open circles) from water/methanol (50/50 v/v %) solutions of pH = 3.5. (b) FTIR analysis of P4VP films adsorbed onto CaF_2 substrates. The absorbance peaks centered at 1600 and 1640 cm^{-1} indicate unprotonated and protonated pyridine ring bands, respectively. Solid lines are absorbance spectra obtained in transmission mode and dotted lines are deconvoluted spectra calculated by the Lorentzian−Gaussian model. In this case, the degree of protonation of P4VP is determined by integrating the peak intensity. (c) Loss in the amount of an adsorbed film of $(PAA/P4VP)_5$ vs pH, as determined by QCM. The prepared multilayer films were immersed in various pH solutions for 24 h and then examined by QCM.

cm^{-1}) and protonated (centered at 1640 cm^{-1}) pyridine rings of P4VP shows that 97% of P4VP is uncharged and only 3% P4VP is protonated at pH 3.5. These results support that the major interaction for buildup of P4VP/PAA multilayers is hydrogen bonding, although electrostatic interaction between COO^- groups (about less than 10% of groups of PAA) and protonated pyridine groups (about 3% of the pyridine groups of P4VP) is possible.

Figure 2c shows the pH stability of hydrogen-bonded multilayer films composed of PAA and P4VP (film structure: $(PAA/P4VP)_5$). These films are stable up to

pH ~7, after which the desorbed amounts sharply increase in the range of pH 7.5−9, with essentially 100% of the film removed at pH 10.3. In a related study, Sukhishvili and Granick reported that hydrogen-bonded PEO/PAA multilayer films assembled in water of pH = 2.0 are rapidly and completely removed upon exposure to solutions above pH 3.6.[40,41] It was also found that the addition of salt (NaCl) provides added pH stability to the multilayer films due to a reduction in the electrostatic repulsions in the layers.[40,41] On the basis of these results, the high pH and broad pH range of deconstruction observed for the P4VP/PAA multilayer films in our work may be influenced by the electrostatic interactions between P4VP and PAA. Additionally, the hydrogen-bonding interactions between PAA and P4VP, as investigated in the current work, are much stronger than those between PAA and PEO, thus accounting for the observed higher pH stability of the films. The higher pH required for decomposing the PAA/P4VP hydrogen-bonded films may also be related to the solvents from which the films were deposited. Dubas et al. reported that the bilayer thickness of PDADMAC/PSS multilayer films prepared from water/ethanol mixtures sharply increases with increasing ethanol content up to 40 wt %, above which PSS starts to precipitate due to the increased hydrophobicity, suggesting the θ condition is to be found near this point.[47] They also suggested that this increase of PE hydrophobicity drives the PE to the interface. Similarly, PAA in methanol/water mixtures precipitates above 90 wt % methanol, as methanol solvent has more hydrophilic character than ethanol. Hence, we cannot exclude the possibility that the water/methanol mixture used for film deposition increases the extent of hydrophobic interactions between the methanol-insoluble PAA and the water-insoluble P4VP at pH 3.5 (and decreases the electrostatic interactions), giving rise to enhanced stability of the multilayer films at a high pH. This effectively contributes to suppressing the deconstruction of hydrogen-bonded layers from electrostatic repulsion between the layers.

Formation of Multilayer Films Based on Hydrogen Bonding and Electrostatic Interactions. Multilayer films composed of hydrogen-bonded and electrostatically assembled layers (e.g., $PE_E/(P_H)_{n=1-4}/PAA/PE_E$ where PE_E = PAH/PSS/PAH and $(P_H)_n$ = $(PAA/P4VP)_n$, $n = 1-4$) were prepared by exploiting the interactions between the two different functional groups within the PAA chains, as schematically shown in Figure 3. The film structure was designed so that the PAA/P4VP layers are physically confined between PAH/PSS/PAH layers. The pH and solvent composition used for film buildup were identical to the conditions employed for preparing the hydrogen-bonded multilayer films (Figure 2).

Figure 4 shows that multilayer film growth occurs, as reflected by the increase in adsorbed amounts (or frequency decrease) with increasing number of both hydrogen-bonded layers and electrostatically assembled layers (i.e., even and odd number of periodic layers, respectively). These results reveal that the deposition of electrostatically interacting layers on top of hydrogen-bonded layers has no significant effect with respect to disrupting the hydrogen bonding between PAA and P4VP. The deposition step for P4VP onto PAA in the $PE_E/(P_H)_1/PAA/PE_E$ film causes a $-\Delta F$ of 75 ± 5 Hz. This is a smaller change in comparison with the 110 ± 5 Hz observed for P4VP deposition in the PAA/P4VP

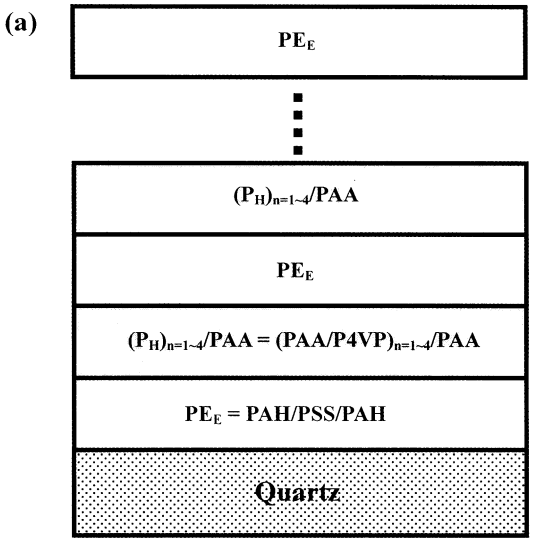

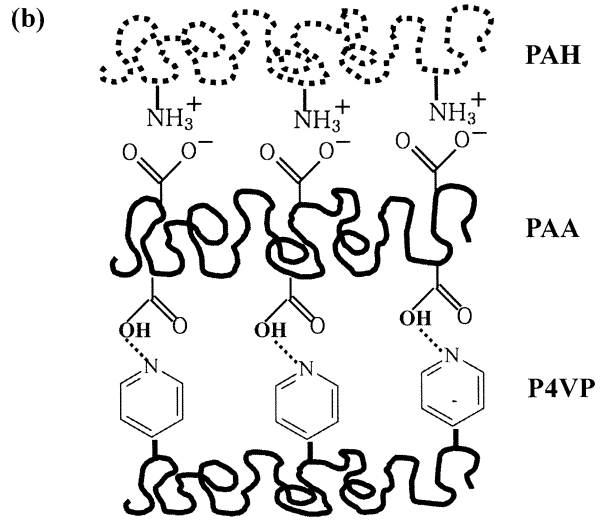

Figure 3. Schematic illustrations of the multilayer films composed of electrostatic and hydrogen-bonded layers. (a) Diagram of the film structure sequence. (b) PAA's role in connecting layers by both electrostatic and hydrogen-bonding interactions, thereby utilizing the nonionized (COOH) and ionized (COO^-) functional groups to promote multilayer formation.

multilayer films presented in Figure 2a. Additionally, for the P4VP deposition step in the $PE_E/(P_H)_{n=1-4}/PAA/PE_E$ films, $-\Delta F$ was also observed to change from 75 for $n = 1$ to 110 Hz for $n = 2$, 3, or 4. We rationalize this increase in adsorbed amount of P4VP in terms of the degree of ionization of the underlying PAA layer onto which P4VP is deposited. Xie and Granick reported that strong PEs (quarternized PVP/PSS) deposited onto a weak PE layer (PMA) cause an oscillation in the ionization degree of the PMA layer from about 30 to 80%.[34,35] Accordingly, in our systems, when PAA is deposited onto PAH/PSS/PAH films (i.e., $n = 1$) (PAH is highly positively charged at pH = 3.5), a proportion of the COOH groups within the adsorbed PAA layer would be converted into COO^- due to the influence of the underlying electrostatically assembled layers (specifically PAH). This PAA layer would therefore be more highly ionized than PAA layers in films where $n = 2-4$,

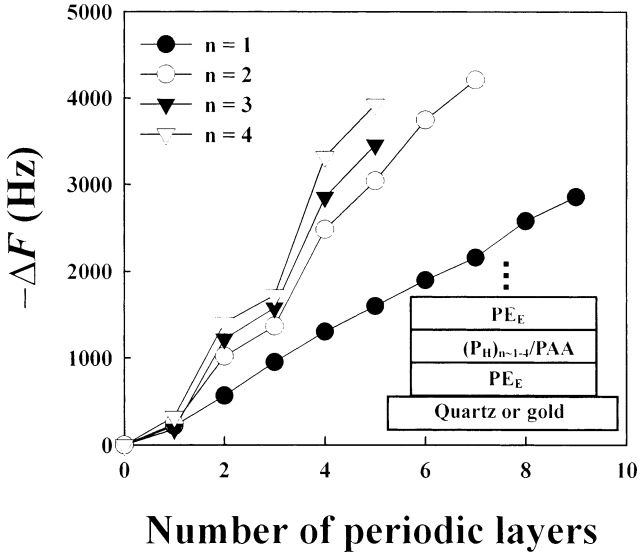

Figure 4. QCM frequency change as a function of the number of periodic layers for the assembly of [PAH/PSS/PAH/(PAA/P4VP)$_{n=1-4}$/PAA]$_m$ (i.e., [PE_E/$(P_H)_{n=1-4}$/PAA]$_m$) from water/methanol (50/50 v/v %) solutions of pH = 3.5. Odd and even number of periodic layers indicate PAH/PSS/PAH (electrostatically assembled layers) and (PAA/P4VP)$_{n=1-4}$/PAA (hydrogen-bonded layers), respectively. The number of inserted hydrogen-bonded layers increases from n = 1 to 4, and PAH/PSS/PAH formed the outermost layers.

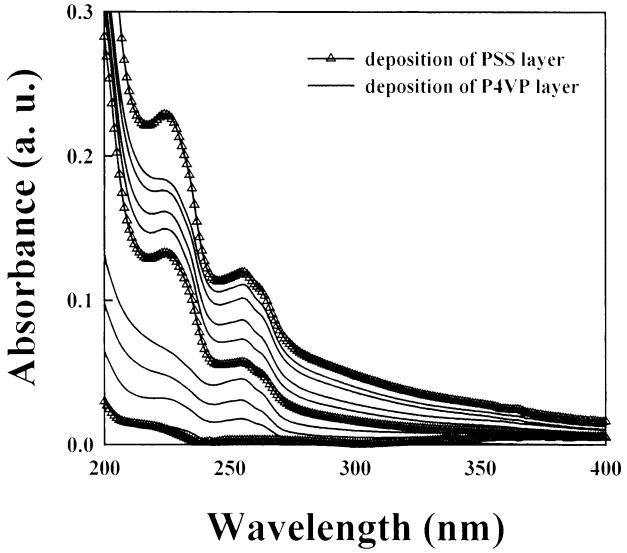

Figure 5. UV−vis absorption spectra of multilayer films with the film structure quartz/[PE_E/$(P_H)_4$/PAA]$_2$/PE_E. The absorbance spectra were measured after the deposition of PE_E and P_H. The absorption peaks at 225 and 256 nm are due to absorption by PSS and P4VP, respectively.

thus decreasing the adsorbed amount of P4VP as a result of less COOH groups being available for hydrogen bonding. That is, increasing the number of hydrogen-bonded layers adsorbed onto electrostatically assembled PE layers reduces the effect of the PAH/PSS layers on the ionization degree of the outer PAA onto which P4VP is adsorbed, resulting in higher P4VP adsorbed amounts.

With increasing PAA/P4VP bilayer number between respective PAH/PSS/PAH layers, the film thickness of inserted hydrogen-bonded layers increases from 4.7 ± 0.2 to 22.7 ± 3 nm (calculated from QCM data) for the PE_E/$(P_H)_1$/PAA/PE_E and PE_E/$(P_H)_4$/PAA/PE_E systems, respectively. Ellipsometric measurements on identical films prepared on silicon wafers revealed similar thicknessses for the hydrogen-bonded layers: 3.8 ± 0.4 (n = 1) and 19.7 ± 0.6 nm (n = 4). This trend was also confirmed by UV−vis spectrophotometry of the four different multilayer films, as indicated in Figure 5. The absorbance peaks at 225 and 256 nm originate from PSS within the electrostatically formed layers and P4VP within the hydrogen-bonded layers, respectively. It should be noted that the increase in film absorbance and the QCM frequency changes (Figure 4) support the formation of strong hydrogen bonding between PAA and P4VP.

Deconstruction Kinetics of Hydrogen-Bonded Multilayer Films Inserted between Electrostatically Assembled Layers. To investigate the deconstruction kinetics of the multilayer films, we measured the change of film absorbance as a function of pH and time for multilayers exposed to solutions of varying pH. First, in the case of five bilayer PAA/P4VP films deposited onto a PAH/PSS/PAH film, the typical absorbance peak of P4VP (at 256 nm) monotonically decreased from pH = 6.8 to 8.5 and essentially completely disappeared at pH = 9.0 in 1 h (Figure 6a). The trend in these data is consistent with the QCM results (Figure 2c). In addition, the absorbance peak of PSS centered at 225 nm reveals that the electrostatically assembled layers are stable, despite the high pH (9.0) used in our experiments. The deconstruction kinetics of [PE_E/$(P_H)_4$/PAA]$_2$/PE_E films at different pH conditions was also investigated (Figure 6b). The film deconstruction characteristics depended sensitively on pH, with both an increase in the rate of film deconstruction and film loss observed with increasing pH from 7.8 to 9.0. This trend is similar to that observed for hydrogen-bonded multilayer films composed solely of PAA and P4VP (Figure 2c). The remaining adsorbed amount (∼25%) for the PE_E/$(P_H)_4$/PAA/PE_E film after 300 min at pH 9.0 is attributed to residual P4VP and the PAH/PSS/PAH layers strongly associated with the quartz substrate (see later). Additionally, as shown in Figure 6c, the physically confined hydrogen-bonded films display different deconstruction kinetics at pH 9.0, depending on the number of inserted hydrogen-bonded layers. At the same pH (9.0), hydrogen-bonded films that are not physically confined between electrostatically assembled layers are almost completely deconstructed (Figure 2c). Increasing the number of inserted hydrogen-bonded layers accelerates the film deconstruction rate, which is accompanied by a larger degree of film loss. These observations can be explained by the diminished interaction of the (intermediate) PAA/P4VP layers with the under- and overlying PAH/PSS/PAH film upon increasing n from 1 to 4, thereby resulting in enhanced release of the hydrogen-bonded layers in response to an increase in pH. As the number of hydrogen-bonded layers between electrostatically assembled layers increases, the deconstruction properties of the physically confined PAA/P4VP layers approach those of nonconfined PAA/P4VP films.

Figure 7 shows the film loss as a function of pH for multilayer films containing physically confined hydrogen-bonded layers. From QCM measurements, the proportion of hydrogen-bonded layers within multilayer films of PE_E/$(P_H)_n$/PAA/PE_E increases from 47 wt % (n = 1) to 83 wt % (n = 4). The PE_E/$(P_H)_1$/PAA/PE_E film (n = 1) is highly resistant to deconstruction up to pH = 8.5, and even at pH 10.3, only 15 wt % of the total film is desorbed. With increasing n, the film stability sharply

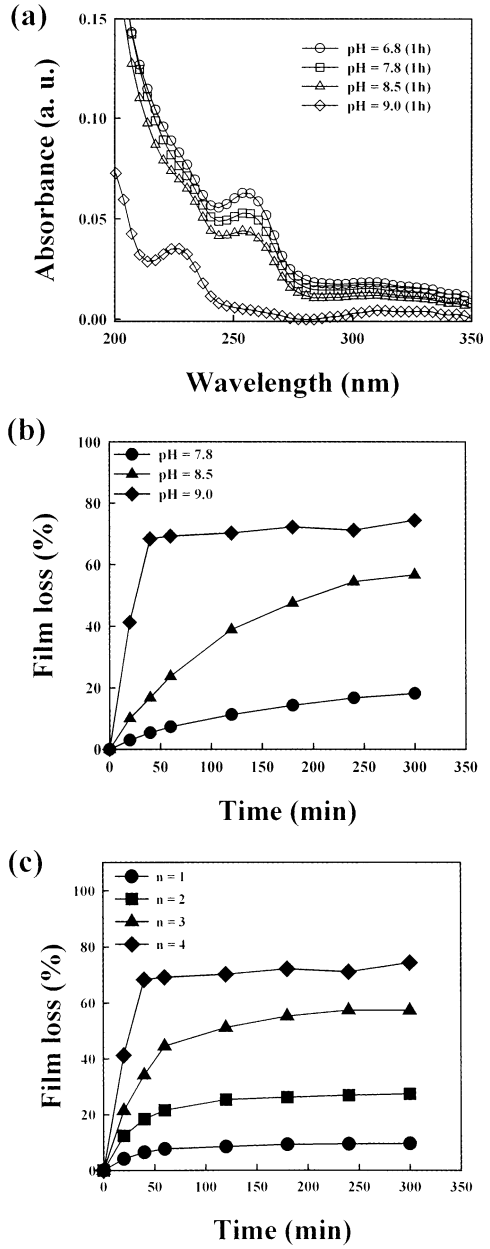

Figure 6. (a) UV−vis absorption spectra of quartz/PE_E/$(P_H)_5$ films after exposure to various pH solutions for 1 h. The quartz substrates used were first coated with PE_E (i.e., PAH/PSS/PAH), and hydrogen-bonded multilayers, P_H (i.e., PAA/P4VP), were subsequently deposited onto the substrates. (b) Deconstruction kinetics of a $[PE_E/(P_H)_4/PAA]_2/PE_E$ film as a function of time at different pH conditions. (c) Deconstruction kinetics of multilayer films as a function of time at pH = 9.0. The film structure is $[PE_E/(P_H)_n/PAA]_m/PE_E$, where $n = 1$, $m = 3$ (●); $n = 2$, $m = 3$ (■); $n = 3$, $m = 3$ (▲); and $n = 4$, $m = 2$ (◆). In parts b and c, the change of the P4VP absorbance peak at 256 nm was followed by UV−vis spectrophotometry.

decreases, yielding a large amount of film loss with increasing pH. In particular, in the case of the PE_E/$(P_H)_4$/PAA/PE_E film, the enhanced film loss in the pH range 7.4−8.5 is similar to that of the pure hydrogen-bonded multilayer films (Figure 2c). However, the PE_E/$(P_H)_4$/PAA/PE_E film cannot be completely removed due to the electrostatically assembled layers first deposited onto the substrate; that is, the 17 wt % of film remaining after exposure to a solution of pH 10.3 is due to the PAH/PSS/PAH layers adsorbed onto the substrate.

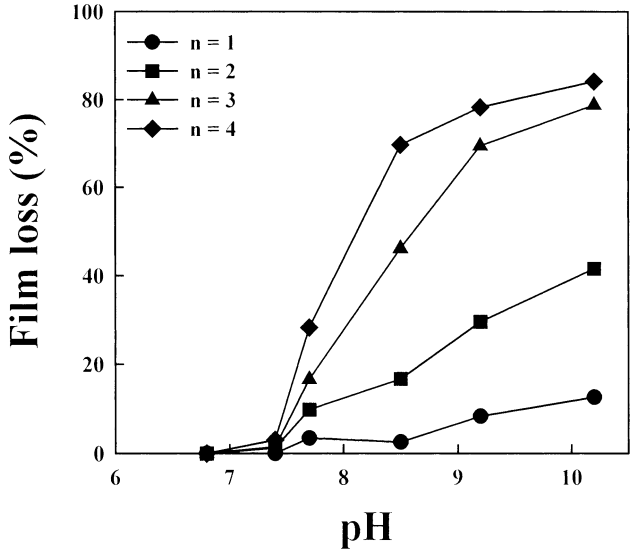

Figure 7. Film loss of the adsorbed amount of $PE_E/(P_H)_n$/PAA/PE_E as a function of pH. Electrostatically assembled PE_E layers formed the outermost layers of the films. The film loss was measured by QCM after immersion in various pH solutions for 24 h.

From a comparison between the initial amounts of adsorbed hydrogen-bonded layers and the total film loss, it is evident that the breakage of hydrogen bonds between PAA and P4VP at high pH decreases the stability of the multilayer films. This process would cause polymer chain swelling and reorganization of the PAA/P4VP layers.[32,46] The breakage of hydrogen bonds in the films is caused by changes in the PAA chain conformation induced by pH changes. In nonionized PAA/P4VP films, the respective PAA layer is adsorbed onto P4VP in the form of loop and tails. An increase in pH eliminates hydrogen-bonding sites by converting COOH into COO^- groups, and at the same time, breaks hydrogen bonds by causing entangled PAA chains to be more extended as a result of intermolecular electrostatic repulsion, and increasing electrostatic repulsion between PAA layers (i.e., intramolecular repulsion). In our system, however, PAA layers within $PE_E/(P_H)_1$/PAA/PE_E films may be suppressed from swelling extensively and structurally reorganizing. This is mainly due to the respective PAA chains that interact through hydrogen bonding with P4VP also electrostatically interact with the PAH/PSS/PAH film, as well as interpenetrating neighboring PEs.[10,29,47]

The pH-sensitive deconstruction characteristics of hydrogen-bonded layers can also be used to prepare free-standing multilayer films. We prepared stacks of PAA/P4VP/PAA separated by PAH/PSS/PAH (see Figure 3a) and subsequently exposed them to high pH conditions (pH ∼10). Atomic force microscopy revealed that the PAH/PSS/PAH layers could be readily separated from the multilayer films (data not shown). This provides an alternative route to the preparation of the free-standing multilayer films composed of electrostatically associating polymers. In a related recent study, Schlenoff and co-workers reported that multiple strata of strong PE multilayer membrane films are produced by removal of intermediate weak PE release layers by exposing the preassembled multilayer films on solid supports to solutions of various ionic strength or pH.[10]

Conclusions

We have demonstrated that the use of carboxylic acid and carboxylate groups coexisting within PAA layers (at pH = 3.5) permits the LbL preparation of multilayer films composed of hydrogen-bonded and electrostatically interacting layers. Designing the structure of the polymeric multilayer films with an increasing number of hydrogen-bonded layers inserted between the electrostatically associated layers converts largely pH-resistant films into erasable multilayer films with adjustable deconstruction kinetics. This pH stability of the hydrogen-bonded layers is strongly influenced by their physical confinement within the stacks of electrostatically interacting layers. In particular, our findings emphasize the pH-controlled stability that can be exerted over multilayer films containing confined hydrogen-bonded layers, without chemical treatment such as thermal or photoinduced cross-linking. This approach represents a facile means to prepare films with tailored deconstruction properties, which may find use in the construction of polymeric multilayered delivery vehicles, membranes, or for patterning surfaces. Additionally, considering that the breakage of the multilayer films originates at the interface between PAA and P4VP, our method can be applied to the fabrication of free membrane films by the use of pH controllable hydrogen-bonded stacks as "release layers" for separating stacks of electrostatically assembled PE multilayers.

Acknowledgment. This work was supported by the BMBF and the Volkswagen Foundation. We thank E. Poptoshev, T. Cassagneau, and B. Schöler for helpful discussions.

References and Notes

(1) Ho, P. K. H.; Kim, J.-S.; Burroughs, J. H.; Becker, H.; Li, S. F. Y.; Brown, T. M.; Cacialli, F.; Friend, R. H. *Nature (London)* **2000**, *404*, 481.
(2) Ho, P. K. H.; Granstrom, M.; Friend, R. H.; Greenham, N. C. *Adv. Mater.* **1998**, *10*, 769.
(3) Fou, A. C.; Onitsuka, O.; Ferreira, M.; Rubner, M. F.; Hsieh, B. R. *J. Appl. Phys.* **1996**, *79*, 7501.
(4) Onitsuka, O.; Fou, A. C.; Ferreira, M.; Hsieh, B. R.; Rubner, M. F. *J. Appl. Phys.* **1996**, *80*, 4067.
(5) Eckle, M.; Decher, G. *Nano Lett.* **2001**, *1*, 45.
(6) Cho, J.; Char, K.; Kim, S.-Y.; Hong, J.-D.; Lee, S. K.; Kim, D. Y. *Thin Solid Films* **2000**, *379*, 188.
(7) Stepp, J.; Schlenoff, J. B. *J. Electrochem. Soc.* **1997**, *144*, L155.
(8) Laurent, D.; Schlenoff, J. B. *Langmuir* **1997**, *13*, 1552.
(9) Caruso, F.; Schüler, C. *Langmuir* **2000**, *16*, 9595.
(10) Dubas, S. T.; Farhat, T. R.; Schlenoff, J. B. *J. Am. Chem. Soc.* **2001**, *123*, 5368.
(11) Balachandra, A. M.; Dai, J.; Bruening, M. L. *Macromolecules* **2002**, *35*, 3171.
(12) Dai, J.; Balachandra, A. M.; Lee, J. I.; Bruening, M. L. *Macromolecules* **2002**, *35*, 3164.
(13) Sullivan, D. M.; Bruening, M. L. *J. Am. Chem. Soc.* **2001**, *123*, 11805.
(14) Jin, W.; Shi, X.; Caruso, F. *J. Am. Chem. Soc.* **2001**, *123*, 8121.
(15) Onda, M.; Ariga, K.; Kunitake, T. *J. Biosci. Bioeng.* **1999**, *87*, 69.
(16) Onda, M.; Lvov, Y.; Ariga, K.; Kunitake, T. *Biotechnol. Bioeng.* **1996**, *82*, 502.
(17) Jiang, X.; Zheng, H.; Gourdin, S.; Hammond, P. T. *Langmuir* **2002**, *18*, 2607.
(18) Clark, S. L.; Montague, M. F.; Hammond, P. T. *Macromolecules* **1997**, *30*, 7237.
(19) Clark, S. L.; Hammond, P. T. *Adv. Mater.* **1998**, *10*, 1515.
(20) Clark, S. L.; Handy, E. S.; Rubner, M. F.; Hammond, P. T. *Adv. Mater.* **1999**, *11*, 1031.
(21) Caruso, F.; Caruso, R. A.; Möhwald, H. *Science* **1998**, *282*, 1111.
(22) Caruso, F.; Lichtenfeld, H.; Möhwald, H.; Giersig, M. *J. Am. Chem. Soc.* **1998**, *120*, 8523.
(23) Caruso, F.; Möhwald, H. *J. Am. Chem. Soc.* **1999**, *121*, 6039.
(24) Caruso, F.; Lichtenfeld, H.; Donath, E.; Möhwald, H. *Macromolecules* **1999**, *32*, 2317.
(25) Caruso, F.; Shi, X.; Caruso, R. A.; Susha, A. *Adv. Mater.* **2001**, *13*, 740.
(26) Caruso, F.; Spasova, M.; Salgueiriño-Maceira, V.; Liz-Marzán, L. M. *Adv. Mater.* **2001**, *13*, 1090.
(27) Gittins, D. I.; Susha, A. S.; Schoeler, B.; Caruso, F. *Adv. Mater.* **2002**, *14*, 508.
(28) Decher, G.; Hong, J.-D.; Schmitt, J. *Macromol. Chem., Macromol. Symp.* **1991**, *46*, 321.
(29) For a review, see: Decher, G. *Science* **1997**, *277*, 1232.
(30) Yoo, D.; Shiratori, S. S.; Rubner, M. F. *Macromolecules* **1998**, *31*, 4309.
(31) Shiratori, S. S.; Rubner, M. F. *Macromolecules* **2000**, *33*, 4213.
(32) Mendelsohn, J. D.; Barrett, C. J.; Chan, V. V.; Pal, A. J.; Mayes, A. M.; Rubner, M. F. *Langmuir* **2000**, *16*, 5017.
(33) Fery, A.; Schöler, B.; Cassagneau, T.; Caruso, F. *Langmuir* **2001**, *17*, 3779.
(34) Xie, A. F.; Granick, S. *J. Am. Chem. Soc.* **2001**, *123*, 3175.
(35) Xie, A. F.; Granick, S. *Macromolecules* **2002**, *35*, 1805.
(36) Wang, T. C.; Rubner, M. F.; Cohen, R. E. *Langmuir* **2002**, *18*, 3370.
(37) Stockton, W. B.; Rubner, M. F. *Macromolecules* **1997**, *30*, 2717.
(38) Wang, L.; Wang, Z. Q.; Zhang, X.; Shen, L. C.; Chi, L. F.; Fuchs, H. *Macromol. Rapid Commun.* **1997**, *18*, 509.
(39) Wang, L.; Fu, Y.; Wang, Z.; Fan, Y.; Zhang, X. *Langmuir* **1999**, *15*, 1360.
(40) Sukhishvili, S. A.; Granick, S. *J. Am. Chem. Soc.* **2000**, *122*, 9550.
(41) Sukhishvili, S. A.; Granick, S. *Macromolecules* **2002**, *35*, 301.
(42) Yang, S. Y.; Rubner, M. F. *J. Am. Chem. Soc.* **2002**, *124*, 2100.
(43) Caruso, F.; Niikura, K.; Furlong, D. N.; Okahata, Y. *Langmuir* **1997**, *13*, 3422.
(44) Schoeler, B.; Kumaraswamy, G.; Caruso, F. *Macromolecules* **2002**, *35*, 889.
(45) Ruths, M.; Sukhishvili, S. A.; Granick, S. *J. Phys. Chem. B* **2001**, *105*, 6202.
(46) Dubas, S. T.; Schlenoff, J. B. *Langmuir* **2001**, *17*, 7725.
(47) Dubas, S. T.; Schlenoff, J. B. *Macromolecules* **1999**, *32*, 8153.
(48) Dubas, S. T.; Schlenoff, J. B. *Macromolecules* **2001**, *34*, 3736.

MA021049N